A TRNSYS model of a direct contact membrane distillation (DCMD) system coupled to a flat plate solar collector (FPC)

4 authors:

Ahmed Remlaoui
Belhadj Bouchaib University -Ain Temouchent
40 PUBLICATIONS   23 CITATIONS

SEE PROFILE

Driss Nehari
Universitaire de Ain Temouchent
82 PUBLICATIONS   259 CITATIONS

SEE PROFILE

Abderrahmane Elmeriah
University Mustapha Stambouli of Mascara
15 PUBLICATIONS   24 CITATIONS

SEE PROFILE

Mohammed Laissaoui
Centre de Développement des Energies Renouvelables
20 PUBLICATIONS   73 CITATIONS

SEE PROFILE

A TRNSYS model of a direct contact membrane distillation (DCMD) system coupled to a flat plate solar collector (FPC)

Ahmed Remlaoui[1]*, Driss Nehari[1], Abderrahmane Elmeriah[1], Mohammed Laissaoui[2]

*1. Smart Structure Laboratory, Unive*rsity Center of Ain-Temouchent
   46000 Ain-Temouchent, Algeria donremlaoui@gmail.com,
   nehari2746@gmail.com elmeriahabderrahmane@gmail.com
2. Centre de Développement des Energies Renouvelables, CDER,
   B.P. 62.Route de l'Observatoire. 16040 Bouzaréah, Algiers, Algeria
   amraoui44@yahoo.fr

RESUME. La présente étude propose un système de dessalement de l'eau prometteur basé sur la distillation par membrane à contact direct (DCMD), alimenté par un capteur solaire à plaque plate (FPC). Le système réalisé est modélisé et simulé à l'aide du code commercial TRNSYS. Cela a été possible en incluant un composant novateur capable de simuler le comportement physique du DCMD. La simulation du système de distillation solaire a été réalisée le 21 juin à 10 heures par le jour dans les conditions météorologiques de la ville de Ain Témouchent (Algérie). Les résultats ont montré que le modèle actuel est en bon accord avec les données expérimentales de la littérature. Le système de dessalement actuel permet d'obtenir une production quotidienne de distillats d'environ 42,86 l / j et le taux de production quotidien spécifique de distillats est de 10,85 kg pour chaque m^2 de FPC. De plus, en ce qui concerne les paramètres de performance, il a été constaté que les fractions solaires allaient de 0 à 1 et que l'efficacité des capteurs était évaluée à 74%.

ABSTRACT. A promising water desalination system based on direct contact membrane distillation (DCMD) powered by flat plate solar collector (FPC) is proposed in the present study. The carried out system is modelized and simulated by using the commercial code TRNSYS. Doing this was possible by including a novel component able to simulate the physical behavior of the DCMD. The simulation of the solar distillation system has been done during the 21st june along a daylight of 10 hours under the meteorological conditions of Ain Témouchent city (Algeria). The results showed that the present model has a good agreement with the experimental data of the literature. The present desalination system allows to get a daily distillate production around 42.86 l/d and the specific daily distillate production rate is 10.85 kg for each m^2 of FPC. Furthermore, concerning the performance parameters, it was found that the solar fractions ranged from 0 to1 and the collector efficiencies was assessed 74%.

Mots-clés : Dessalement solaire, distillation membranaire directe, capteur solaire plant, traitement de l'eau, TRNSYS.

KEYWORDS: Solar desalination, direct contact membrane distillation, flat plate solar collector, water treatment, TRNSYS.

1. Introduction

Southern Mediterranean countries are facing a growing water scarcity. This shortage induces the need to increase the water supply via alternative sources. Rural and remote areas are particularly uncomfortable because they are often far from the municipal water systems and conventional sources, and often they are not connected with the electricity grid. There are opportunities to address the problem of water scarcity in rural and remote areas through sustainable saltwater desalination technologies.

The desalination of seawater and brackish water is well-established industry consisting of a wide range of available technologies with decades of experience. Rural and remote region have specific needs, which imposes on us the choice of appropriate technologies.This includes a technical requirements related to a small-scale application using renewable sources of easy operation and maintenance. According to the little scale seawater desalination, the membrane distillation (MD) can be a great option especially in view of the possibility to use the solar thermal and low-grade heat directly as the primary source of energy (R. Schwantes *et al.*, 2013 ; M. Khayet., 2013).

Membrane Distillation is a half process that consolidates both thermal and membrane process. The Membrane has a direct contact with a seawater on the feed side and a fluid or vaporous stage on the permeate side. Therefore, can be characterized as a procedure for expelling water vapor from aqueous feed solution heated to a temperature under 100 °C. The transfer force of the process is the difference in partial pressures between two sides of the membrane, which causes evaporation on the feed side (R. Schwantes *et al.*, 2013 ; M. Khayet *et al. et al.*, 2013;Amir Bahmanyar *et al.*, 2012 ; B.B. Ashoor *et al.*, 2016). Contingent upon the procedure arrangements, four different systems of MD have been distinguished (Amir Bahmanyar *et al.*, 2012 ; B.B. Ashoor *et al.*, 2016): Direct Contact Membrane Distillation (DCMD) where a cold liquid is in coordinate contact with the layer at the permeate side; Air Gap Membrane Distillation (AGMD) where a stagnant air gap is kept up between the membrane and condensing surface; Vacuum Membrane Distillation (VMD) where a pump is employed to make the vacuum on the permeate side and subsequently the condensation happens outside the membrane module; and Sweep Gas Membrane Distillation (SGMD) in which the inert gas is typically used to sweep the vapors at the permeate side and after that to condense these vapors outside the membrane module.

Among the previous cited configurations, DCMD is the most widely considered due to the straightforwardness to setup and the adequately high flux rate in examination with other MD configurations. In addition, membrane distillation is less membrane-fouling problem than the systems that use pressure as the reverse osmosis (RO) (Mohammed Laissaoui *et al.*, 2018). There are many modeling and experimental investigations of complex processes during DCMD operation including heat and mass transfer, operating parameters effects, pore size distribution air flux, flow rate, flow velocities and feed temperature have been reported in the literatures (Tsung-Ching Chen *et al.*, 2009 ; M.A. Izquierdo-Gila *et al.*, 2008; J. Phattaranawik *et al.*, 2003).

Several experimental works dealing with solar desalination systems have been done. Among them, Francisco Suárez *et al.* (2015) whose carried out an experimental inquiry to decide the freshwater production rates and energy requirements of the coupled DCMD with salt-gradient solar pond (SGSP) system. The results showed that the average fresh water flux outputted is 1.0 L.hr^{-1}m^{-2} of membrane which is equivalent to 1.16 10^{-3} m^3/d per m^2 of solar pond, in the other side, the DCMD/SGSP system produces a sustainable water flux approximately six times greater than the AGMD/SGSP system operating under similar conditions. Furthermore, 70% of the energy extracted from the SGSP was used to drive the thermal desalination and the rest was lost in various areas of the system.

The experimental investigation of R. Gemma Raluy *et al.* (2012) presented a solar compact MD installed in Playa de Pozo Izquierdo (Gran Canary Island-Spain). Their results was obtained during 5 year experiment and data analysis demonstrated that the unit water production was ranged from 5 to 120 L/d and specific thermal energy consumption (STEC) was between 140 and 350 kWh/m^3. Fawzi Banat *et al.*(2007) manufactured a little scale solar membrane desalination unit (SMADES) with the plant coordinates solar thermal and photovoltaic energy. The feed water is specifically warmed by solar thermal collector and afterward exchanged to spiral-wound AGMD module. The main results showed that the plant worked consistently up to 120 L/d, STEC was in the scope of 200-300 kWh/m^3 and the solar collector efficiency reached 45 %.

Concerning the hypothetical examinations in view of operating parameters influence on the permeate flux, W.G. Shim *et al.*(2015) developed a mathematical model to predict permeate flux inside solar-DCMD system for seawater desalination which was studied under unsteady conditions, different types of polytetrafluoroethylene (PTFE) membranes, membrane properties (liquid inlet pressure "LEP", pore diameter, porosity and pore size distribution) were characterized for each membrane. The results have given a good agreement between a numerical simulation and experimental outcomes, the experimental STEC ranged from 896 kWh/m^3 to 1433 kWh/m^3 and the Gain output ratio (GOR) ranged from 0.44 to 0.70. The solar-DCMD system has been operated in Korea for more than 150 days of seawater desalination; while during the day, more than 77.3 % of the solar energy is supplied to the heating. Otherwise, Jianhua Zhang *et al.*(2011) implemented a simple mathematical model designed to incorporate the effects of membrane length, temperature and flow rate of feed fluid on flux of co-current and counter flow DCMD, based on the mass transfer coefficients and heat transfer coefficients obtained directly from the experimental results. The authors found a reasonable agreement with the experimental results.

Amongst the most vital programming used as a part of this field, there is the transient system simulation program (TRNSYS) that used to simulate the solar-DCMD process in order to develop and improve this domain, where few simulations have been carried out. Hung C. Duong *et al.*(2017) developed a TRNSYS model to simulate the performance of an integrated solar thermal driven direct contact membrane distillation (DCMD) framework for seawater desalination utilizing

recorded climate information from 1st to 5th January 1991 in New South Wales Australia. A spiral-wound DCMD module connected to solar thermal collector composed of 10 flat. The results obtained from the simulation showed that distillate production is subject to the accessibility of solar radiation amid the day; in any case, a little framework can deliver more than 140 kg of distillate every day under genuine climate conditions. Gowtham Mohan *et al.*(2016) present a dynamic modeling using the TRNSYS simulator program to aim evaluate a new solar thermal polygeneration (STP) system for cold creation by single stage LiBr-H2O chiller absorption, clean water (MD) and Domestic hot water is investigated with three diverse solar collectors - flat plate collectors (FPC), evacuated collector tube (ETC) and compound parabolic collector (CPC) for the climate conditions of the United Arab Emirates (UAE). The outcomes demonstrated that the most minimal recuperation time of 6.75 years is accomplished by STP with an ETC field with a gross zone of 216 m^2.

Juan Pablo Vargas-Bautista *et al.*(2017) have experimentally evaluated the thermal, environmental and economic performance of a small-scale ethanol distillation system using solar energy by evacuated solar collector tube (ETC) and parabolic trough collectors (PTC) system with two different concentrations of ethanol at the feed stream (5 wt.% and 10 wt.%) were tested to acquire a distillate product of 95 wt.% ethanol (hydrous ethanol).The thermal analysis of the simulation demonstrated that PTC represents a superior choice, where 80% and 71% of the energy investment funds can be accomplished by 5 % wt and 10% wt of ethanol respectively in the sustain stream. Luis Acevedo *et al.*(2016) built up a dynamic model TRNSYS to design a providing power system by coupling photovoltaic/thermal collectors (PVT) and a wind turbine (WT), the aim of this study is to produce a domestic hot water (SHW) from PVT and ETC and freshwater (FW) that obtained through two seawater desalination systems (MD and RO), whereas a new type of MD system has been integrated in TRNSYS program. The primary outcomes showed that the MD system produced up to 15,311 L/year and cover an electrical energy request of 1890 kWh. Moreover, the system outputted SHW, FW and power coverage by 99.3 %, 100 % and 70 % consecutively.

From recent studies (R. Schwantes *et al.,*2013; R. Gemma Raluy *et al.,*2012; Fawzi Banat *et al.,*2007; Parimal Pal *et al.,*2010), the authors reported only the solar driven DCMD motionless seawater desalination systems, which supplies nearby areas with potable water. Nevertheless, requires financial liquidity to supply the surrounding areas from the station site. In this case, there is a huge need to use a solar-DCMD system mobile. Through extensive existing studies of small-scale solar-DCMD system, which requires a small value of hot water and thus can be achieved in areas with a medium temperature following the literatures (Hung C. Duong *et al.,*2017; Fawzi Banat *et al.,*2008; A.E. Kabeel *et al.,*2017).

The previous studies lacked to give complete simulations of a solar energy and DCMD systems that allows finding the optimization of a little scale seawater solar desalination, which can be useful for mobile DCMD solar installations with production of drinking water. The objective of the present study is to conduct numerically a mobile small size system with DCMD for brackish water desalination and application in order to provide the areas which are far from drinking water sources

and electric power, whereas the combination of the solar energy systems is used to produce simultaneously the thermal energy for heating the brackish water and desalinated water. According to that, the following technologies are in the same time incorporated into the system: Solar brackish water Heating system with FPC and DCMD for desalination. This numerical inquiry includes; (i) creation of a novel TRNSYS component of DCMD system by Fortran software, (ii) heat and mass transfer analysis through the membrane ; (iii) Assess the performance of the solar thermal driven DCMD process.

2. Mathematical Modelling

2.1. Membrane modeling

The membrane distillation process is governed by different heat and mass transfer formularizations that occur at both feed side of the membrane and permeate side. The mass transfer occurs through the pores of the membrane while the heat is transferred through both the membrane and its pores.

Fig.1 shows a 2D schematic plan of DCMD heat and mass transfer mechanism, the mass flux J_w (L.m^{-2}.hr^{-1}) of water can be written as a linear function of the vapor pressure difference across the membrane and the membrane mass transfer coefficient B_m (L.m^{-2}.hr^{-1}.Pa^{-1}) (J.Phattaranawik et $al.,$2003; M.Qtaishat et $al.,$2008; F. Eleiwi et $al.,$2016) given by:

$$J_w = B_m(P_{mf} - P_{mp}) \qquad (1)$$

Where P_{mf} and P_{mp} are the partial pressures in feed and permeate sides (Pa) as a function of the temperature on the feed (T_{mf}) and permeate (T_{mp}) at the membrane surface (^{o}C) that can be calculated with Antoine equation:

$$P_{mf,p} = \exp(23.1964 - \frac{3816.44}{T_{mf,p}+227.04}) \qquad (2)$$

The heat transfer involved in DCMD can be divided into three regions (B.B. Ashoor et $al.,$2016; F. Eleiwi et $al.,$2016):

(1) Convective thermal transfer in the feed boundary layer .

(2) The combination of the conduction heat transfer across the membrane and the heat transferred due to the migration of water vapor through the pores of the membrane(M.H. Sharqawy et $al.,$2010).

(3) Convective thermal transfer in the permeate boundary layer.

In the stationary state, the overall flow of heat transfer Q (W.m^{-2}) across the entire DCMD system is given by(V.A. Bui et $al.,$2010):

$$Q = (\frac{1}{h_f} + \frac{1}{h_m + \frac{j_w \Delta H_v}{T_{mf} - T_{mp}}} + \frac{1}{h_p})^{-1}(T_{bf} - T_{bp}) \qquad (3)$$

As a result, the overall heat transfer coefficient U (W.m^{-2}K^{-1}) for the DCMD process is expressed as follows(V.A. Bui et $al.,$2010):

$$U = \left(\frac{1}{h_f} + \frac{1}{h_m + \frac{j_w \Delta H_v}{T_{mf} - T_{mp}}} + \frac{1}{h_p}\right)^{-1} \tag{4}$$

In the equations above, h_f is the feed boundary layer heat transfer coefficient (W.m^{-2}K^{-1}), h_p is the permeate boundary layer heat transfer coefficient (W.m^{-2}K^{-1}), ΔH_v is the latent heat of vaporization (J.L^{-1}) (M.H. Sharqawy *et al.*,2010) [24], h_m is the thermal transfer coefficient of the hydrophobic membrane (W.m-2K-1) which can be calculated from the membrane thermal conductivity k_m (W.m^{-1} K^{-1}) (Amir Bahmanyar *et al.*,2012) [3] and δ_m the membrane thickness (m).

The temperatures T_{mf} and T_{mp} at the surfaces of the membrane can be estimated as (Amir Bahmanyar *et al.*,2012; M.H. Sharqawy *et al.*,2010; L. Martinez-Diez *et al.*,1999):

$$T_{mf} = \frac{k_m\left(T_{bp} + \frac{h_f}{h_p}T_{bf}\right) + \delta_m(h_f T_{bf} - J_w \Delta H_v)}{k_m + h_f(\delta_m + \frac{k_m}{h_p})} \tag{5}$$

$$T_{mp} = \frac{k_m\left(T_{bf} + \frac{h_p}{h_f}T_{bp}\right) + \delta_m(h_p T_{bp} + J_w \Delta H_v)}{k_m + h_p(\delta_m + \frac{k_m}{h_f})} \tag{6}$$

Where T_{bf} and T_{bp} are the bulk temperature on the feed and permeate sides (K).

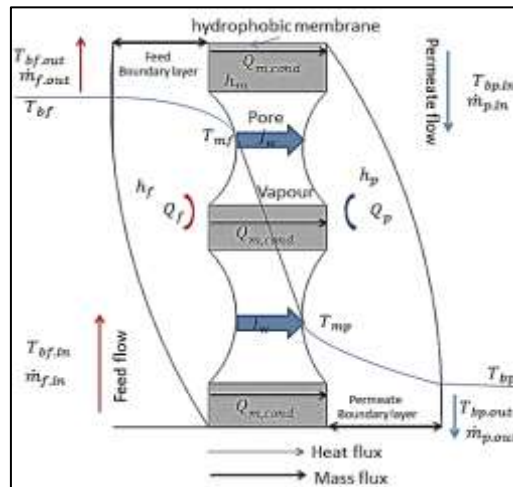*Figure 1. Heat and mass transfer through a DCMD membrane.*

A simple model based on the mass transfer coefficient C_{global}(L.hr^{-1}.m^{-2}.pa^{-1}) and overall heat U (J.hr^{-1}m^{-2}K^{-1}) related membrane properties to verify the effect of membrane length, temperature and velocity on the heat and mass flow. This model has been compared to the experimental and modelling results of Jianhua Zhang *et al.*(2011) by using the mass transfer coefficient and global heat at the same flow rate as present following the adjustment equations (Jianhua Zhang *et al.*,2011) :

$$U = -5248V^2 + 4735.7V - 36.036 \tag{7}$$

$$C_{global} = -0.004V^2 + 0.0053V - 0.0001 \tag{8}$$

For simplify the model, it is assumed that (Jianhua Zhang *et al.,*2011):

➢ The heat exchanged to the environment through the wall of the module can be ignored.

➢ As indicated by R. G. Lunnon. (1912), the latent heat of evaporation and condensation does not change with concentration.

➢ C_{global} And U are constant for a given membrane at a steady rate.

➢ There is no temperature slope across the membrane perpendicular to the direction of flow.

➢ By adjusting the mass exchange, the permeate mass going through the membrane can be neglected.

➢ By balancing the heat transfer, the sensible heat passed by the permeate can be neglected. As indicated by these assumptions, the mass flux can be expressed as follows:

$$J_w = C_{global}(P_{bf} - P_{bp}) \tag{9}$$

Where P_{bf} and P_{bp} are the partial pressures of the water (Pa) respectively as a function of the temperature on the feed side T_{bf} and permeate side T_{bp} ; these pressures are defined as follows (W.G. Shim *et al.,*2015):

$$P_{bf,p} = \exp\left(23.1964 - \frac{3816.44}{T_{bf,p}+227.04}\right) \tag{10}$$

Fig.2 shows the heat and mass transfer of a co-current DCMD in a flat sheet module, the heat change in the hot side, cold side and membrane can be described as follows (Jianhua Zhang *et al.,*2011):

$$C_{p,f}\dot{m}_f(T_{f,i+1} - T_{f,i}) = -[U(T_{f,i} - T_{p,i})dA + J_w\Delta H_v dA] = C_{p,p}\dot{m}_p(T_{p,i} - T_{p,i+1}) \tag{11}$$

$C_{p,f}$ And $C_{p,p}$ are the feed and permeate specific heat capacity (kJ.kg^{-1}K^{-1}),dA = wdx where A membrane area (m^2), w is the membrane width (m), the feed temperature change is calculated as:

$$\Delta T_{f,i} = -\frac{[U(T_{f,i}-T_{p,i})+J_w\Delta H_v]wdx}{C_{p,f}\dot{m}_{f,i}} \tag{12}$$

The permeate temperature change is calculated as:

$$\Delta T_{p,i} = \frac{[U(T_{f,i}-T_{p,i})+J_w\Delta H_v]wdx}{C_{p,p}\dot{m}_{p,i}} \tag{13}$$

C_{global} And U are assumed to be constants, the feed and permeate temperatures at the $(i + 1)^{th}$ station can be calculated by:

$$T_{f,i+1} = T_{f,i} - \Delta T_{f,i} \tag{14}$$

$$T_{p,i+1} = T_{p,i} - \left(\frac{m_f}{m_p}\right)\Delta T_{f,i} \tag{15}$$

The mass and heat flux transfer at the $(i + 1)^{th}$ station can be determined as follows:

$$J_{i+1} = C_{global}\left(P_{f,i+1} - P_{p,i+1}\right) \tag{16}$$

$$Q_{i+1} = U\left(T_{f,i+1} - T_{p,i+1}\right) \tag{17}$$

From which the total mass and heat flux transfer of the membrane can be calculated as:

$$J = \frac{\sum_{i=0}^{N} J_i W \Delta x}{A} \tag{18}$$

$$Q = \frac{\sum_{i=0}^{N} Q_i W \Delta x}{A} \tag{19}$$

The algorithms calculations of the DCMD procedure are given in Fig. 3 for co-current. The computation begins from the feed inlet end ($x_0 = 0$) and completions at the concentrate outlet end ($x_N = L$) of the DCMD module.
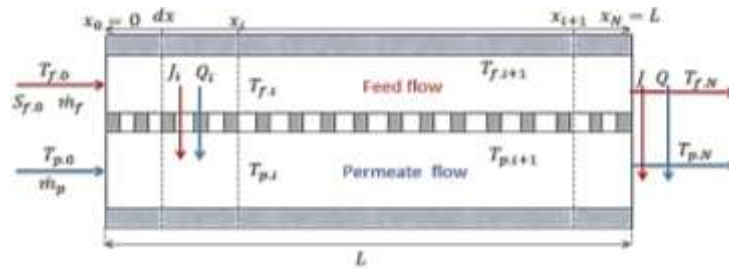
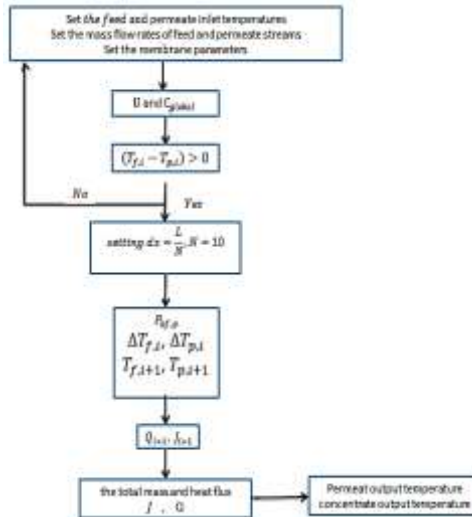Figure 2. The heat and mass transfer of a co-current DCMD in a flat sheet module.

Figure 3. The algorithms calculations of the DCMD model for co-current flow.

2.2. Solar distillation system

The proposed model for freshwater production from brackish water and thermal energy is a combination of direct Contact Membrane Distillation (DCMD) and flat plate solar collector (FPC) as shown in Fig 4. The fundamental solar distillation system is made out of solar thermal collector, auxiliary heater, heat exchanger, pump and DCMD module.

The thermal energy is provided from a solar collector which captures the solar energy transmitted by radiation and transferred it to the heat transfer fluid (in the present we use propylene glycol, that its $Cp=3.708$ $kJ.kg^{-1}.K^{-1}$) in the form of heat; these heat transfer fluids coming into contact with a counter current tubular heat exchanger to transfer its heat to the brackish water and to ensure an ideal temperature for the DCMD process is used an auxiliary heater. The system consists mainly of principal subsystems:

(1)   Solar thermal loop.
(2)   The DCMD module.
(3)   Power loop (production, regulation and consumption).

The heat transfer fluid (HTF) is assumed as an extremely huge part in a solar collector system. In a SBH (solar brackish water heating) framework, HTF absorbs the thermal energy in the collector and transmits it through the heat exchanger to the brackish water. The HTF properties such as boiling and solidification point, flash point, viscosity, and thermal capacity assume a part in the choice of a working liquid for a SBH system. For instance, a SBH system individually will require a HTF with a low freezing point and a high boiling point in cold and hot climates. The most portion of the regular HTFs utilized are air, water, hydrocarbon oils, Glycol/water blend, and refrigerants/stage change fluids (Ruchi Shukla *et al.,*2013).
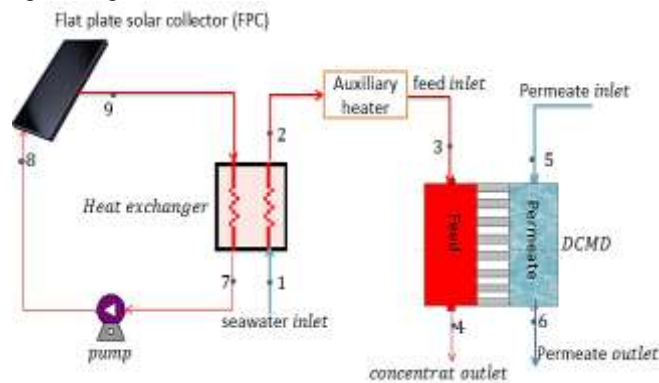

Figure 4. Schematic diagram of the solar DCMD system.

2.2.1. Flat plate solar collector (FPC)

The solar thermal collectors utilize the accessible solar energy to heat an HTF. The following equations are the basic equations for the useful collector energy and for the collector efficiency (Juan Pablo Vargas-Bautista *et al.,*2017; Fei Cao *et al.,*2014).

$$Q_u = \dot{m}_{fs} C_{p,fs} (T_9 - T_8) \tag{20}$$

Where Q_u presents the heat collected by solar collector ($Kj.hr^{-1}$), T_8 and T_9 are the inlet and outlet temperature of the solar fluid (K), $\dot{m}_{fs}$ is the solar fluid mass flow rate ($kg.hr^{-1}$) and $C_{p,fs}$ is the specific heat capacity of solar fluid ($kJ.kg^{-1}K^{-1}$)

The solar collector thermal efficiency η_{coll} can be expressed by the following equation (Gowtham Mohan *et al.,*2016):

$$\eta_{coll} = \frac{Q_u}{A_c \, G_T} = \eta_0 - a_1 \frac{(T_{av} - T_{amb})}{G_T} - a_2 \frac{(T_{av} - T_{amb})^2}{G_T} \tag{21}$$

Where G_T is the incident total solar radiation ($kJ.hr^{-1}.m^{-2}$), A_c is the collector gross area (m²), η_0 is the optical efficiency, a_1 is the global heat loss coefficient ($kJ.hr^{-1}.m^{-2}.K^{-1}$) and a_2 is the temperature dependence of the global heat loss coefficient ($kJ.hr^{-1}.m^{-2}.K^{-2}$); T_{amb} Ambient temperature (°C) and T_{av} is the average collector fluid temperature (°C). Such parameters are accessible for tried collectors that obtained experimentally and generally given by the maker and associations capable of confirming these values.

2.2.2. Auxiliary heater

The chosen auxiliary devices are important to supply additional heating energy to the proposed systems. Generally these apparatus are an electric auxiliary heater supplied via photovoltaic (PV) power, which is a source of continuous electrical energy that converted into an alternating current using an inverter. The excess energy produced is stored in batteries. The radiator is intended to add heat to the seawater at a rate not exactly or equivalent to Q_{max} ($kJ.hr^{-1}$). The auxiliary heater operation is described from the rate of heat addition to the brackish water Q_{fluid} ($kJ.hr^{-1}$), the thermal rate losses from heater to environment Q_{loss} ($kJ.hr-1$) and required heating rate including efficiency effects Q_{aux} ($kJ.hr^{-1}$) (Juan PabloVargas-Bautista *et al.,*2017):

$$Q_{fluid} = \dot{m}_{bw} C_{p,bw} (T_{set} - T_2) \tag{22}$$

$$Q_{loss} = UA(\bar{T} - T_{env}) + Q_{max}(1 - \eta_{aux}) \tag{23}$$

With: $\bar{T} = \frac{T_3 + T_2}{2}$

$$Q_{aux} = Q_{fluid} + Q_{loss} \tag{24}$$

Where $\dot{m}_{bw}$ brackish water mass flow rate ($kg.hr^{-1}$), $C_{p,bw}$ brackish water specific heat ($kJ.kg^{-1}.K^{-1}$), UA overall loss coefficient between the heater and its surroundings during operation ($kJ.hr^{-1}$), T_{set} set temperature of heater internal thermostat (C), T_{env} temperature of heater surroundings for loss calculations (°C), T_2 and T_3 are the inlet and outlet brackish water temperature (°C), $\bar{T}$ brackish water average temperature (°C) and η_{aux} efficiency of auxiliary heater.

The solar fraction SF (or solar share), represent the ration of the provided energy by the solar collector to the totale required energy for the fonctioning of desalination system(Juan PabloVargas-Bautista *et al.,*2017; Fei Cao *et al.,*2014)is in this way:

$$SF = \frac{Q_u}{Q_u + Q_{aux}} \tag{25}$$

2.2.3. Heat exchanger

In Solar brackish water Heating system, the heat exchanger (HX) is utilized to transfer absorbed solar heat from the working fluid to the brackish water. The counter flow heat exchanger is included in modeling of the system. Below is the general equation for calculating the steady-state heat transfer in the heat exchanger:

Total heat transfer rate across heat exchanger P_{hx} (kJ.hr^{-1}) is calculated by (Jantaporn Waritha *et al.,*2017) :

$$P_{hx} = UA\ LMTD = \dot{m}_{bw}C_{p,bw}(T_2 - T_1) = \dot{m}_{fs}C_{p,fs}(T_7 - T_9) = \varepsilon_{hx}\dot{m}_{bw}C_{p,bw}(T_9 - T_1) \tag{26}$$

Whereas UA overall heat transfer coefficient of exchanger (kJ.hr^{-1}), $\dot{m}_{bw}C_{p,bw}$ capacity rate of fluid on cold side (kJ.hr^{-1}), $\dot{m}_{fs}C_{p,fs}$ capacity rate of fluid on hot side (kJ.hr^{-1}), T_1 and T_2 are the brackish water inlet and outlet temperature (C), T_9 and T_7 are the solar fluid inlet and outlet temperature (C) and LMTD the logarithmic mean temperature difference (Jantaporn Waritha *et al.,*2017).

Heat exchanger effectiveness ε_{hx} is calculated by (A.E. Kabeel *et al.,*2017):

$$\varepsilon_{hx} = \frac{1 - exp\left(\frac{-UA}{\dot{m}_{bw}C_{p,bw}}(1 - \frac{\dot{m}_{bw}C_{p,bw}}{\dot{m}_{fs}C_{p,fs}})\right)}{1 - \frac{\dot{m}_{bw}C_{p,bw}}{\dot{m}_{fs}C_{p,fs}}exp\left(\frac{-UA}{\dot{m}_{bw}C_{p,bw}}(1 - \frac{\dot{m}_{bw}C_{p,bw}}{\dot{m}_{fs}C_{p,fs}})\right)} \tag{27}$$

2.2.4. Direct contact membrane distillation (DCMD)

The efficiency of a desalination plant in view of distillation is characterized regarding consumed of thermal energy. There are two primary definitions to introduce this efficiency: Gain output ratio (GOR) is defined as the ratio between the evaporation latent heat ΔH(kJ.kg^{-1}) (L. Martinez-Diez *et al.,*1999) multiplied by the distilled water produced $\dot{m}_d$ (kg.hr^{-1}) and the heat input to the system Q_{input} (kJ.hr^{-1}) (R. Gemma Raluy *et al.,*2012; A.E. Kabeel *et al.,*2017; H.C.Duong *et al.,*2015).

$$GOR = \frac{\dot{m}_d \Delta H}{Q_{input}} \tag{28}$$

3. System simulation using TRNSYS

3.1. TRNSYS model

The system described in the previous section was dynamically simulated by transient systems simulation (TRNSYS 17). Every component model is subroutines ("Type") that exists in the standard library of TRNSYS. Table 1 demonstrates the

devices and the corresponding simulation subroutine (Type). Once all the components of the system have been identified and a mathematical description of each component is available, the main components of this model are described and shown in Table 1.

Tableau 1. The components of the Transys17 simulation programs.

Component	Type
Flat plate solar thermal collector	TYPE73
Pump	TYPE110
Weather data reading and processing	TYPE15-6TM2
Heat exchanger	TYPE5b
Auxiliary heater	TYPE6
Control signal	TYPE14h
Mains brackish water supply profile	TYPE14h
Mains freshwater supply profile	TYPE14h
Mains brackish water supply temperature	TYPE14e
Mains freshwater supply temperature	TYPE14e
DCMD	New TRNSYS component- TYPE223
Online plotter	TYPE65c
Integrator	TYPE24
Printer	TYPE25c

TRNSYS software is utilized for analyzing the performance of the system, as the whole system is modeled as shown in Fig. 5.

Flat plate collectors (FPC) are simulated using the Type 73 model available in the TRNSYS library. TRNSYS simulation program is employing the standard second-order collector performance. Type110 model is a variable speed pump that can keep up any outlet mass flow rate in the vicinity of zero and uttermost value. The mass flow rate of the pump differs directly with control signal setting. The fluid solar is pumped from 8 am to 6 pm consistently. We have to force the mass flow rate on the pump by sending a period changing control signal with Type14h.

Type 14 forcing functions were utilized few times in the model to enter mains brackish water and freshwater supply temperature (Type 14e), mains brackish water and freshwater supply profile (Type 14h) and control signal. The process was operated at constant distillate water circulation rates (36 L/hr) and distillate temperature (25°C), the feed water circulation flow rates of this module shown in Fig. 6 and the feed water temperature (25 °C).

The auxiliary heater (Type 6) has an extreme power of 1388.9 W and losses of charge not to be considered. The set point is 60°C. The climate data TM2 (Typical Meteorological File) used is the one of the region of Ain Temouchent-Algeria. The

simulation of the solar distillation system consists of 10 h per day; in this study the representatif day selected to done the simulation was 21st jun.
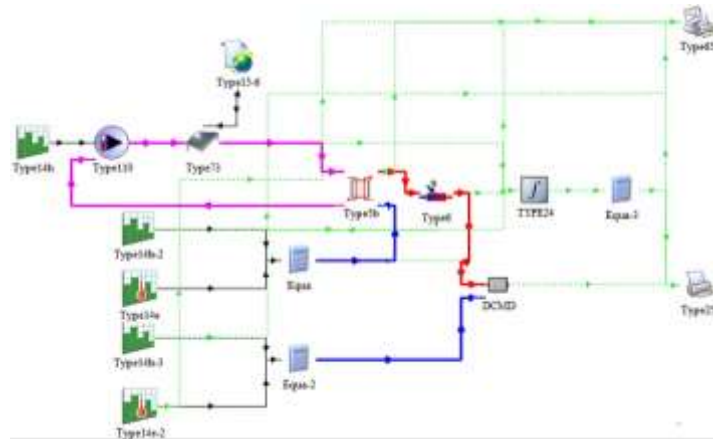

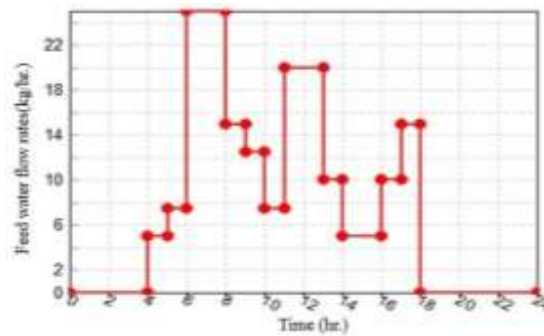*Figure 5. Solar thermal and DCMD systems modeled in TRNSYS 17.*

Figure 6. Feed water load variation during the day.

Tables 2, 3 and 4 show parameters values of the auxiliary heater, pump and solar collectors respectively used in the TRNSYS model.

Tableau 2. Input parameters of the auxiliary heater for TRNSYS simulation.

Parameters	Value	Unit
Maximum heating rate	5000	$kJhr^{-1}$
Specific heat of fluid	4.190	$kJkg^{-1}K^{-1}$
Overall loss coefficient for heater during operation	0	$kJhr^{-1}K^{-1}$
Efficiency of auxiliary heater	1	-
The set point temperature	60	°C

Tableau 3. Main input parameters of the Flat plate solar collector for TRNSYS simulation(L.M. Ayompe et al.,2011).

Parameters	Value	Unit
Number in series	2	-
Collector absorber area	3.95	m^2
Fluid specific heat	3.708	$kJkg^{-1}K^{-1}$
Tested flow rate	80	$kghr^{-1}m^{-1}$
Intercept efficiency	0.776	-
First order efficiency coefficient	14.22	$kJhr^{-1}m^{-2}K^{-1}$
Second order efficiency coefficient	0.0594	$kJhr^{-1}m^{-2}K^{-2}$
Maximum flow rate	212	$kghr^{-1}$
Collector slope Degrees	53	Degrees
Absorber plate emittance	0.7	-
Absorbance of absorber plate	0.8	-
Number of covers	1	-
Index of refraction of cover	1.526	-
Extinction coefficient thickness product	0.28	-

Tableau 4. Input parameters of pump for TRNSYS simulation (L.M. Ayompe et al.,2011).

Parameters	Value	Unit
Rated flow rate	212	$Kg.hr^{-1}$
Fluid specific heat capacity	3.708	$kJ.kg^{-1}K^{-1}$
Rated power	226.8	$kJ.hr^{-1}$

3.2. Creation of a DCMD type in TRNSYS envirement

The simulation run using TRNSYS17 software has been executed via injected a new programed component; in particular TYPE 223 is added to the standard library. This new TYPE is committed to a desalination unit DCMD. This component is written by FORTRAN language. Table 5 shows a various parameters values for the DCMD model.

Tableau 5. Parameters for the DCMD model(Jianhua Zhang et al.,2011).

Parameters	Value	Unit
Membrane material	PTFE	-
Membrane length	0.145	m
Pore size	1	µm
Contact angle	126	Degrees

membrane area	0,0136	m^2
membrane Width	0.1	m
Specific heat of freshwater	4190	J.kg^{-1}K^{-1}
Specific heat of feedwater	4190	J.kg^{-1}K^{-1}
feed water speed	0.4	m.s^{-1}
Salinity	10	gNaCl.Lwater^{-1}

4. results and discussion

4.1.Validation of the DCMD model

In order to validate our numerical predictions based on the new TRNSYS component (DCMD unit); we have studied the system designed by Jianhua Zhang.(2011) from co-current configurations for a velocity of 0.4 m.s^{-1}. The cold inlet temperature was kept constant at 20 °C and the hot inlet temperature is assumed higher than 60 °C, the Perspex module with membranes different lengths were used here. Fig. 7 shows the comparison between the given experimental results (Jianhua Zhang., 2011) and the numerical results obtained from the model used in the present investigation. It can be noticed that the permeate flux predicted by the present model has a good agreement with the experimental data. The average difference between the permeate fluxes provided by the present model (modeling) and experiment is 8% for the Membrane effective length at 0.07 m. This discrepancy between predicted permeates fluxes and experimental data is also find by Jianhua Zhang.(2011) and could be justified by : the experimental error and different empirical equations which are used for the modeling.
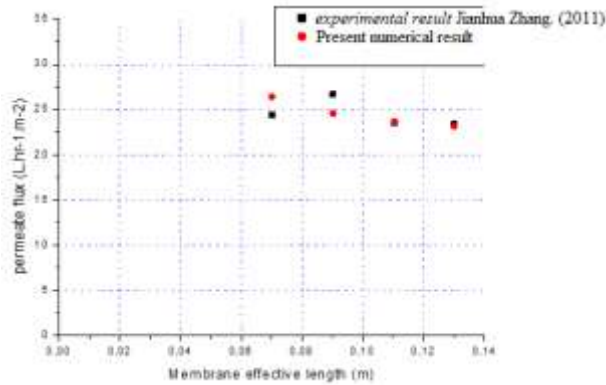

Figure 7. Validation of the numerical model at (T5=20°C, T3=60°C, V=0.4m.s-1) with Jianhua Zhang. (2011) *experimental result.*

The model was also verified with temperature profile. Fig. 8 shows the comparison between the given numerical results (Jianhua Zhang *et al.,*2011) and the present numerical results wich use the same numerical model. It is clear that the both numerical results fit well, as they are from the same analytic model. In this figure (Fig.

8), the temperature profile of the feed side and the permeate side along the membrane module in co-current flow mode are depicted under the following conditions: The permeate temperature (T5) of 20˚C, the inlet feed temperature (T3) of 60˚C ; flow velocity of the fluids 0.4 m.s^{-1} and the PTFE membrane effective length is 0.145 m. These results predict local temperatures on both sides of the membrane approach each other at different lengths of membranes. From the plot, we notice that the temperature of permeate side is increasing, in contrast of the feed side which is decreasing. Moreover, the temperature gradient between the fluid on both sides is converged from the inlet to the outlet of the membrane.
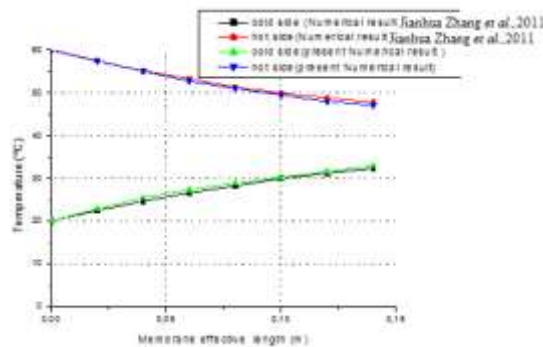
Figure 8. Validation of the numerical model at: (L=0.145 m ,V=0.4m/s, T5=20°C and T3=60°C)

4.2. Results and discussion for the solar distillation system

In order to run a simulation for the selected represetatif day (Jun 21st), in the subject to predict the performance of the SBH system, a typical Meteorological Year of Ain Temouchent (TMY) is used at GMT1 time zone, latitude 35.306 ^{0}N and longitude -1.147 ^{0}E were used. Fig. 9 demonstrates the variation of hourly values of solar radiation, ambient temperature and wind speed. The most extreme estimations of solar radiation was 920 W.m^{-2} during this day. The greatest ambient temperatures was 29.45°C.
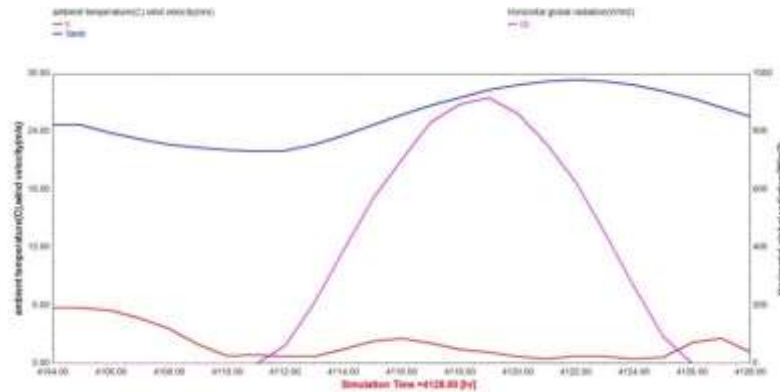
Figure 9. Solar radiation, ambient temperature and wind speed during the day 21ˢᵗ June.

Fig. 10 shows the plots of the mass flow rate and the solar fluid temprature trough the heat exchanger, .And also the solar fluid temperature in the inlet (T8) and outlet (T9)of FPC respectively (see Fig.4).

In this system, the HTF (propylene glycol, Fraction of glycol=0.4, Cp=3.708 kJ.kg^{-1}.K^{-1}) flow usually be through the collector loop by forced convection according to a variable speed pump, where the maximum mass flow rate of the HTF is assumed as constant value 100 kg.hr^{-1} during the function time period of the pump. Various results are obtained from these plots as follow:

    (1) The solar radiation and ambient temperature have a positive effect on the HTF temperature that has reached the uttermost value of 79.44°C at the outlet of FPC in the tested days.

    (2) A temperature curve at the pump inlet applies entirely to the temperature curve at its outlet; in the fact this is due to the objective of pump works to lifting the flow velocity, not to change the HTF temperature. The highest value for them is 76.36 °C.

    (3) The mass flow rate variation has a positive influence on SF.

    (4) One of the most important factors that contribute to increase the temperature is the use of new type HTF fluid with a low freezing point and a high boiling point in cold and hot climates, increase in the collector gross area or change the HTF mass flow rate with solar radiation.
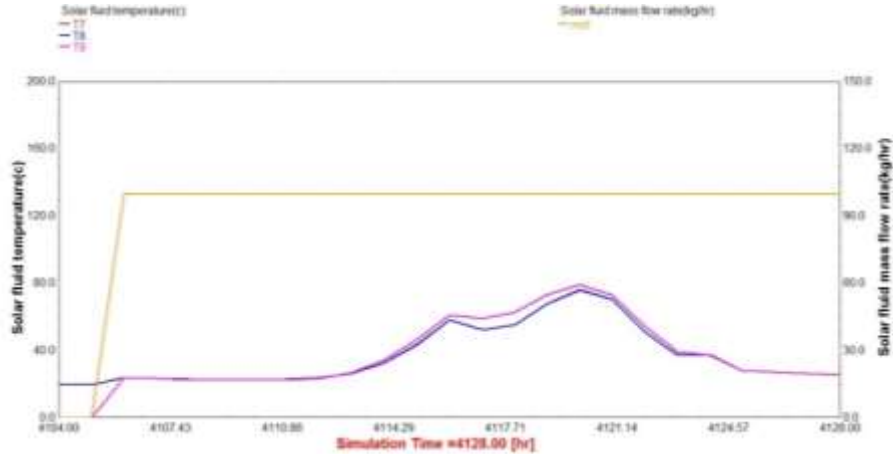
Figure 10. Solar fluid mass flow rate and temperatures for the FPC system in the tested days.

Fig. 11 illustrates the energy of the solar radiation (GT) and the energy supplied by the solar collector (Qu) that is provided to HTF and energy provided by the auxiliary heat to the brackish water (Q_{aux}) for each hour during the 21st June. The results of the simulation indicate during the time interval 8am to 6pm that the solar energy fluctuated in the range 121.97 kJ.hr^{-1}.m^{-2}-1040.26 kJ.hr^{-1}.m^{-2} and the energy supplied by the solar collector is between 8.58 kJ.hr^{-1} and 2783.25 kJ.hr^{-1}, whereas the auxiliary heating consumed a highest value of 2763.59 kJ.hr^{-1}. This means that the high value of the solar radiation leads to minify the intervention of the auxiliary heater to augment the brackish water temperature until 60 °C. From this plot it appears that the auxiliary energy reaches very high values, this is due to that the fluid solar is pumped from 8 am (equivalently 4112 hr) to 6 pm (equivalently 4122 hr). Thus, the energy provided to the brackish water from 6 am (equivalently 4122 hr) to reach the temperature 60 °C is purely from the electric heater.
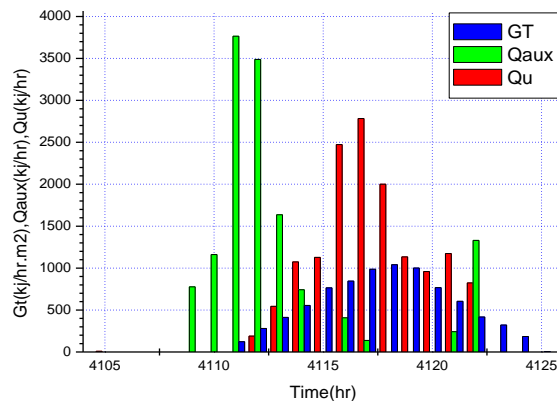

Figure 11. The solar radiation (GT), the energy supplied by the solar collector (Q_u) and the auxiliary heat to the brackish water (Q_{aux}) for a specific time (June 21st) for
$$T_3 = 60\ °C,\ T_5 = 25\ °C.$$

According to the Fig.12, the solar fraction SF, the heat exchanger effectiveness ε_{hx} and the solar collector thermal efficiency η_{coll} for the FPC systems are presented. The SF is in the range $0 \leq SF \leq 1$, the solar savings fraction get zero '0' value for no solar energy utilization, and have the value 1 when the energy is provided only via solar way. For intermediate values different from 0 and 1, the pump and auxiliary heater work together. Conerning solar collector thermal efficiency η_{coll} , its maximum value in our case is 0.74 (i.e. 74%). This value is in concordance with the common value in range 60-80% for most thermal solar collectors. The heat exchanger effectiveness ε_{hx} is also confined between 0 and 1, representing the ratio of energy converted from the working fluid to the seawater and the maximum possible heat transfer rate for the given flow and temperature conditions. The zero value signifies the period intermission of the pump work, whereas for the value 1, the solar fluid energy is transferred to the seawater.
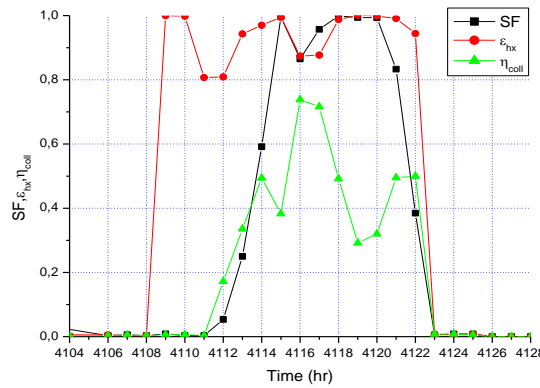

Figure 12. Solar fraction SF*, heat exchanger effectiveness* ε_{hx} *and FPC efficiencie* η_{coll}.

Fig. 13 shows the total heat transfer rate across heat exchanger and the power consumed by the pump for each hour during the 21st June. It can be seen that the power consumed by the pump P_{pump} remains constant and equal to 226.8 kJ.hr^{-1}, this is because the solar fluid mass flow rate is constant within the closed cycle. The total heat transfer rate across heat exchanger P$_{hx}$ is ranged between 565.49 kJ.hr^{-1} and 2795.13 kJ.hr^{-1}, this parametre is proportionnelly to the solar radiation variation. In addition, in the first half daylight between 8am to 14pm (4110 hr to 4116 hr) , the P$_{hx}$ increasing until reach a hight value and this due to the rise of Q$_u$ of solar fluid. Whereas, for the second half daylight from the time 4117 hr, the P$_{hx}$ decreases due to diminution of solar radiation and Q$_u$.
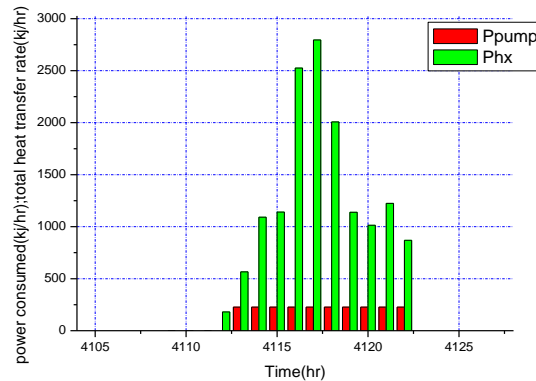
Figure 13. Total heat transfer rate across heat exchanger and the power consumed by the pump for characteristic day

Fig. 14 displays the variation of the useful collector energy, the energy supplied by of auxiliary heater, heat transfer rate across heat exchanger and the power of pump during the 21st June. It appears the same behavior obtained previously in Fig. 11 and 13. It is clear that when the solar radiation ratio is high, the useful heat collected by solar collector is above the auxiliary heat added by electric heater, this leads to raise the solar fraction. However, the use of the auxiliary heat during the solar radiation weakness allows the reduction of the solar fraction and a high energy added to brackish water to reach the the needed temperature of the MD (60 °C).

Concerning the profil of temperature and mass flow rate along the desalination unit (shown in Fig. 4), the cycle starting from the input of the heat exchanger (T_1) that is constant 25 °C, but inside the tubes of heat exchanger, the seawater absorbs the useful energy loaded in the HTF which leads to increase the temperature to the extremely value (T_2) of 60 °C . Most of the time, the brackish water temperature remains below the value required to be distilled, therefore it is heated by auxiliary heater until reaches the temperature at least 60°C and moore than 80°C at output (T_3). After that, the brackish water loses energy inside DCMD system, causing a decrease of brackish water temperature T_4 at outlet feed side and increase of freshwater temperature T_6 at outlet permeate side from 25 °C to 36.15 °C (which has been introduced at a steadfast temperature T_5 of 25 °C).

The mass flow rate highest values of the permeate and concentrate were 36.10 kg.hr^{-1} and 24 kg.hr^{-1} respectively. These values are significantly higher; therefore can be reused with brine recycling or with multi-stage DCMD system.
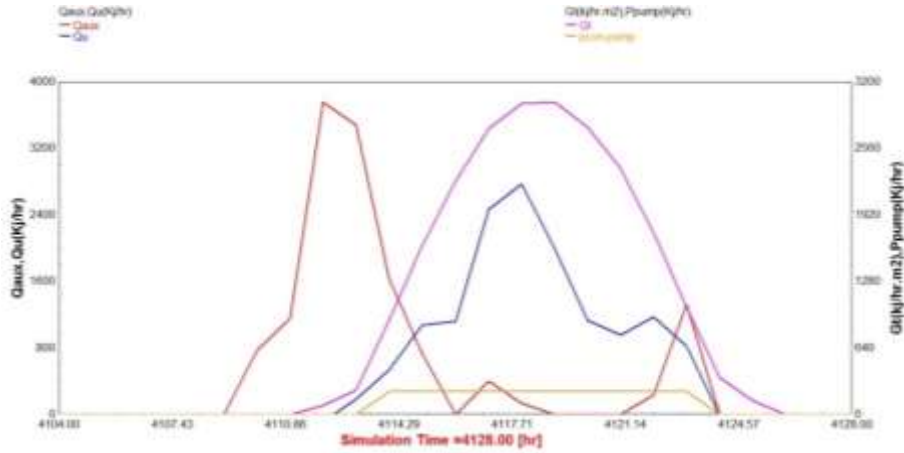
Figure 14. Variation of the the useful collector energy, the energy supplied by of auxiliary heater, the heat transfer rate across heat exchanger and the power of pump (June 21st) for $T_3 = 60$ °C , $T_5 = 25$ °C.

The Fig. 15 presents the temperatures variations at inlet and outlet (T_4 and T_6) of DCMD system, then the total mass and heat flux transfer of the membrane during a summer day (June 21st). At feed side, the brackish water inlet temperature (T_3) is in the range 60-79.22°C (not shown here). The brackish water outlet temperature (T_4) fluctuates in range 43-25°C. Thus, at permeate side, freshwater inlet temperature (T_5) was about 25 ℃ and outlet one (T6) varies from 25 °C to 36.15 °C. The maximum production flux of the permeate is 6.955 L.hr^{-1}. The quality of the total heat flux transfer through the membrane was high 3.15 107 KJ.hr^{-1}m^{-2}.

Referring to the simulation results obtained from the current solar DCMD model, it is observed that are comparable with previous studies as shown in table 6. The distillate production per membrane area reaches its highest value compared with plants with other technolgies membrane (see table 6). On the other hand the distillate production per collector area is in the range of other types of membrane (see table 6). It can be also noted that we have used the collector area and the membrane area less small compared to those of the studies shown in table 6. However, values of daily distillate production of the present study is 42.86 l/d, which is so important for such means that used in the present investigation.
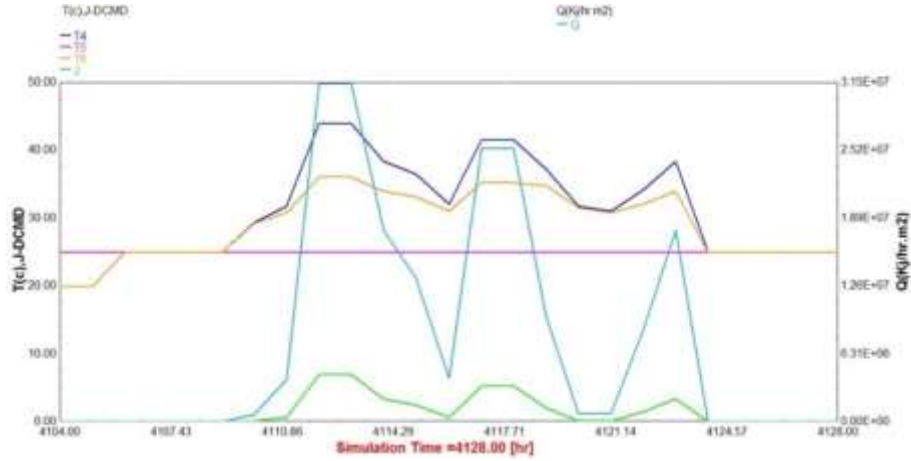
Figure 15. Variation of temperatures curves at inlet and outlet of DCMD system, the permeate total mass flow (gk/hour) and heat flow transfer of the membrane with time during 21st June.

Tableau 6. Comparisons between the simulated DCMD system and the data from the literature.

	Simulated data from the present study	Pilot data from the literature			
		(Hung C. Duong et al.,2017)	(Fawzi Banat et al.,2007)	(H.E.S. Fath et al.,2008)	(J. Koschikowski et al.,2003)
Configurations	flat-sheet DCMD module	spiral-wound DCMD module	PGMD (permeate gap membrane distillation)	PGMD	AGMD
Membrane area (m^2)	0.0136	7.2	10	-	8
Thermal collector area (m^2)	3.95	22.6	5.73	5.73	5.9
Daily distillate production (kg/d)	42.86	142	<120	64.17	81
Distillate production/collector area (kg/(m^{2}d) collector)	10.85	6.3	<20.9	11.2	13.7

Fig. 16 illustrates the Gain output ratio GOR of DCMD system. It is an important parameter in the thermal desalination processes. Typically, in the DCMD processus the value of GOR ranges from 0.3 to 6 according to the literature (Fawzi Banat *et al.,*2007; W.G. Shim *et al.,*2015). It depends on many parameters, such as feed water inlet temperature and feed flow rate. Indeed, the simulation results show that the GOR change from 0 to 0.95 and its average value reached 0.19 .The GOR is related to the solar radiation and varied from one day to another (Fawzi Banat *et al.,*2007).
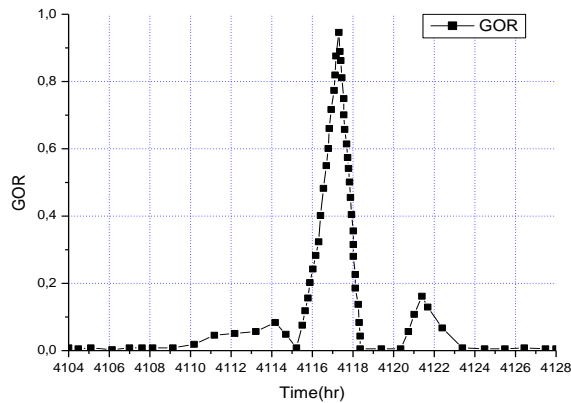

Figure 16. Efficiencies and performance parameters (June 21st),

4. CONCLUSIONS

This study present an analysis of combined solar thermal system and direct contact membrane distillation (DCMD) to produce the freshwater.

In the fact, this process is an alternative to countries that lack drinking water but contain a large amount of salt water and continuous solar radiation during the year. In this paper, a transient simulation software TRNSYS has been used for flat plate solar collector (FPC) powering a small scale DCMD unit, this software allows to evaluate the system over the year. For this purpose, a new TRNSYS component type of DCMD system has been built and added in TRNSYS library as type 223. This study has been realized in special wearther conditions for the Ain Temouchent city, Algeria.

According to that, this type was been included in the scheme with other additional components required for the solar desalination system. The simulation consists of 10h during the 21st June as a typical day in order to evaluate the thermal behaviors of the desalination system.

The average difference between the permeate fluxes provided by the present model and experiment of the literature is 8% for the Membrane effective length at 0.07 m. The proposed solar DCMD system has shown favorable potential application in desalination of brackish water. However, a TRNSYS simulation result was showed that the greatest ambient temperatures was 30 °C, the peak Total horizontal radiation can reach the value 1012 $W.m^{-2}$ in July. In particular, during June 21st, the solar energy fluctuated in the range 121.97 $kJ.hr^{-1}.m^{-2}$ to 1040.26 $kJ.hr^{-1}.m^{-2}$ (33.88 $W.m^{-2}$ to

288.96 W.m^{-2}) and the system was able to generated between 8.58 kJ.hr^{-1} and 2783.25 kJ.hr^{-1} of heat whereas the auxiliary heating consumed a highest value of 2763.59 kJ.hr^{-1} to augment the brackish water temperature from the 60°C. The HTF temperatures reached the highest value of 79.44°C at the outlet of FPC. The pump consumed 226.8 kJ.hr^{-1} and the total heat transfer rate across the heat exchanger ranges between 565.49 kJ.hr^{-1} and 2795.13 kJ.hr^{-1}. Solar thermal driven DCMD system can produce 42.86 kg in June 21st of drinking water. This is equivalent to a daily distillate production rate of 10.85 kg for each m^2 of FPC. In addition to that, the performance parameters which are the solar fractions ranged from 0 to1 and the GOR change from 0 to 0.95 and its average value reached 0.19 where the collector efficiencies was assessed 74 %.

acknowledgment

References

R. Schwantes, A. Cipollina, F. Gross, J. Koschikowski, D. Pfeifle, M. Rolletschek, V. Subiela. (2013). Membrane distillation: solar and waste heat driven demonstration plants for desalination. *Desalination*, vol. 323, p. 93-106. https://doi.org/10.1016/j.desal.2013.04.011

M. Khayet. (2013). Solar desalination by membrane distillation: dispersion in energy consumption analysis and water production costs (a review). *Desalination*, vol. 308, p.89–101. http://dx.doi.org/10.1016/j.desal.2012.07.010

Amir Bahmanyar, Morteza Asghari, Nafiseh Khoobi. (2012) . Numerical simulation and theoretical study on simultaneously effects of operating parameters in direct contact membrane distillation. *Chemical Engineering and Processing*, vol. 61, p. 42-50.http://dx.doi.org/10.1016/j.cep.2012.06.012

B.B. Ashoor,S.Mansour, A. Giwa, V. Dufour,S.W.Hasan. (2016) . Principles and applications of direct contact membrane distillation (DCMD):A comprehensive review. *Desalination,* vol. 398, p. 222-246.http://dx.doi.org/10.1016/j.desal.2016.07.043

Mohammed Laissaoui, Patricia Palenzuela, Mohamed A. Sharaf Eldean, Driss Nehari,Diego-César Alarcón-Padilla. (2018). Techno-economic analysis of a stand-alone solar desalination plant at variable load conditions. *Applied Thermal Engineering,* vol. 133, p. 659-670.https://doi.org/10.1016/j.applthermaleng.2018.01.074

Tsung-Ching Chen, Chii-Dong Ho, Ho-Ming Yeh. (2009). Theoretical modeling and experimental analysis of direct contact membrane distillation. *Journal of Membrane Science*, vol. 330, n° 1, p. 279-287.http://dx.doi.org/10.1016/j.memsci.2008.12.063

M.A. Izquierdo-Gila,C.Fern´andez-Pineda, M.G. Lorenz. (2008). Flow rate influence on direct contact membrane distillation experiments: Different empirical correlations for Nusselt number. *Journal of Membrane Science*, vol. 321,p. 356-363. http://dx.doi.org/10.1016/j.memsci.2008.05.018

J. Phattaranawik, R. Jiraratananon, A.G. Fane. (2003). Effect of pore size distribution and air flux on mass transport in direct contact membrane distillation. *Journal of Membrane Science,* vol. 215, n° 1, p. 75-85.http://dx.doi.org/10.1016/S0376-7388(02)00603-8

Francisco Suárez, Jeffrey A. Ruskowitz, Scott W. Tyler, Amy E. Childress. (2015). Renewable water: Direct contact membrane distillation coupled with solar ponds. *Applied Energy*, vol. 158, p. 532-539.http://dx.doi.org/10.1016/j.apenergy.2015.08.110

R. Gemma Raluy, Rebecca Schwantes, Vicente J. Subiela, Baltasar Peñate,Gustavo Melián, Juana Rosa Betancort. (2012). Operational experience of a solar membrane distillation demonstration plant in Pozo Izquierdo-Gran Canaria Island (Spain). *Desalination*, vol. 290, p. 1-13.http://dx.doi.org/10.1016/j.desal.2012.01.003

Fawzi Banat, Nesreen Jwaied, Matthias Rommel, Joachim Koschikowski,Marcel Wieghaus. (2007). Desalination by a "compact SMADES" autonomous solar powered membrane distillation unit. *Desalination*, vol. 217, p. 29-37. http://dx.doi.org/10.1016/j.desal.2006.11.028

W.G. Shim, K. He, S. Gray, I.S. Moon. (2015). Solar energy assisted direct contact membrane distillation (DCMD) process for seawater desalination. *Separation and Purification Technology*, vol. 143, p. 94-104. https://doi.org/ 10.1016/j.seppur.2015.01.028

Jianhua Zhang , Jun-De Li, Stephen Gray. (2011). Researching and modelling the dependence of MD flux on membrane dimension for scale-up purpose. *Desalination and Water Treatment,* vol. 31, p. 144-150.http://dx.doi.org/10.5004/dwt.2011.2373

Hung C. Duong, Lei Xia, Zhenjun Ma, Paul Cooper, Wendell Ela and Long D. Ngh iem.(2017). Assessing the performance of solar thermal driven membrane distillation for seawater desalination by computer simulation. *Journal of Membrane Science,* vol. 542 n° 1, p. 133-142. http://dx.doi.org/10.1016/j.memsci.2017.08.007

Gowtham Mohan, Uday Kumar, Manoj Kumar Pokhrel, Andrew Martin. (2016). A novel solar thermal polygeneration system for sustainable production of cooling, clean water and domestic hot water in United Arab Emirates: Dynamic simulation and economic evaluation. *Applied Energy*, vol. 167, p. 173-188.http://dx.doi.org/10.1016/j.apenergy.2015.10.116

Juan Pablo Vargas-Bautista, Alejandro Javier García-Cuéllar, Santiago L. Pérez-García,Carlos I. Rivera-Solorio. (2017). Transient simulation of a solar heating system for a small-scale ethanol-water distillation plant: Thermal, environmental and economic performance. *Energy Conversion and Management*, vol. 143, p. 347-360. http://dx.doi.org/10.1016/j.enconman.2016.12.0410196-8904

Luis Acevedo, Javier Uche, Alejandro Del Almo, Fernando Círez, Sergio Usón,Amaya Martínez,Isabel Guedea.(2016).Dynamic Simulation of a Trigeneration Scheme for Domestic Purposes Based on Hybrid Techniques. *Energies*, vol. 9, n° 12, p. 1013.; http://dx.doi.org/10.3390/en9121013

Parimal Pal, Ajay K. Manna. (2010). Removal of arsenic from contaminated groundwater by solar-driven membrane distillation using three different commercial membranes. *water research*, vol. 44, n° 1, p. 5750-5760.http://dx.doi.org/10.1016/j.watres.2010.05.031

Fawzi Banat, Nesreen Jwaied.(2008). Economic evaluation of desalination by small-scale autonomous solar-powered membrane distillation units. *Desalination*, vol. 220, p. 566-573.http://dx.doi.org/10.1016/j.desal.2007.01.057

A.E. Kabeel, Mohamed Abdelgaied, Emad M.S. El-Said.(2017). Study of a solar-driven membrane distillation system: Evaporative cooling effect on performance enhancement. *Renewable Energy,* vol. 106, p. 192-200.http://dx.doi.org/10.1016/j.renene.2017.01.030

J.Phattaranawik,   R. Jiraratananon, A.G.Fane.(2003). Heat transport and membrane distillation coefficientin direct contact membrane distillation. *Journal of Membrane Science*, vol. 212, p. 177-193.https://doi.org/10.1016/S0376-7388(02)00498-2

M.Qtaishat, T.Matsuura, B.Kruczek, M.Khayet. (2008). Heat and mass transfer analysis in direct contact membrane distillation. *Desalination*, vol. 219, p. 272-292.http://dx.doi.org/10.1016/j.desal.2007.05.019

F. Eleiwi , Noreddine Ghaffour, Ahmad S. Alsaadi, Lijo Francis, Taous Meriem Laleg-Kirati. (2016). Dynamic modeling and experimental validation for direct contact membrane distillation (DCMD) process. *Desalination*, vol. 384, n° 1, p. 1-11. http://dx.doi.org/10.1016/j.desal.2016.01.004

M.H. Sharqawy, J.H. Lienhard, S.M. Zubair. (2010).Thermophysical properties of seawater: a review of existing correlations and data. *Desalination and Water Treatment*, vol. 16, p. 354-380.http://dx.doi.org/10.5004/dwt.2010.1079

V.A. Bui, L.T.T. Vu, M.H. Nguyen. (2010). Modelling the simultaneous heat and mass transfer of direct contact membrane distillation in hollow fibre modules. *Journal of Membrane Science*, vol. 353, p. 85-93.http://dx.doi.org/10.1016/j.memsci.2010.02.034

L.   Martinez-Diez , M.I.   Vazquez-Gonzalez.(1999). Temperature and concentration polarization in membrane distillation of aqueous salt solutions. *Journal of Membrane Science*, vol. 159, p. 265-273.https://doi.org/10.1016/S0376-7388(98)00349-4

R. G. Lunnon.(1912). The Latent Heat of Evaporation of Aqueous Salt Solutions. *Proceedings of the Physical Society of London*,p. 18.http://iopscience.iop.org/1478-7814/25/1/317

Ruchi Shukla, K. Sumathyn, Phillip Erickson, Jiawei Gong. (2013). Recent advances in the solar water heating systems: A review. *Renewable and Sustainable Energy Reviews*, vol. 19, n° 1, p. 173-190. http://dx.doi.org/10.1016/j.rser.2012.10.048

Fei Cao , Liang Zhao , Fan Zhang & Liejin Guo.(2014). Redesign of a Water Heating System Using Evacuated Tube Solar Collectors: TRNSYS Simulation and Techno-Economic Evaluation. *Heat Transfer Engineering*, vol. 35, p. 556-566. http://dx.doi.org/10.1080/01457632.2013.837369

Jantaporn, Waritha, Ali, Aamer, Aimar, Pierre.(2017). Specific energy requirement of direct contact membrane distillation. *Chemical Engineering Research and Design*, vol. 128, p. 15-26.https://doi.org/10.1016/j.cherd.2017.09.031

H.C. Duong, Paul Cooper, Bart Nelemans, Tzahi Y. Cath, Long D. Nghiem. (2015). Optimising thermal efficiency of direct contact membrane distillation by brine recycling for small-scale seawater desalination. *Desalination*, vol. 374, p. 1-9. http://dx.doi.org/10.1016/j.desal.2015.07.009

L.M. Ayompe, A. Duffy, S.J. McCormack, M. Conlon. (2011). Validated TRNSYS model for forced circulation solar water heating systems with flat plate and heat pipe evacuated tube collectors. *Applied Thermal Engineering,* vol. 31, p. 1536-1542. http://dx.doi.org/10.1016/j.applthermaleng.2011.01.046

Jianhua Zhang. (2011). *Theoretical and experimental investigation of membrane distillation*.Thèse en of Philosophy, Institute for Sustainability and Innovation, School of Engineering & Science, Victoria University.

H.E.S. Fath, S.M. Elsherbiny, A.A. Hassan, M. Rommel, M. Wieghaus, J. Koschikowski, and M. Vatansever. (2008). PV and thermally driven small-scale, stand-alone solar desalination

systems with very low maintenance needs.*Desalination*,vol. 225, p. 58-69. https://doi.org/10.1016/j.desal.2006.11.029

J. Koschikowski, M. Wieghaus, and M. Rommel. (2003). Solar thermal-driven desalination plants based on membrane distillation. *Desalination,* vol. 156, p. 295-304. https://doi.org/10.1016/S0011-9164(03)00360-6

Article reçu le : AR_1religne_soumission

Article accepté le : AR_soumission